# Projective-Plane Iteratively Decodable Block Codes for WDM High-Speed Long-Haul Transmission Systems

Ivan B. Djordjevic, Sundararajan Sankaranarayanan, and Bane V. Vasic, *Senior Member, IEEE*

***Abstract*—Low-density parity-check (LDPC) codes are excellent candidates for optical network applications due to their inherent low complexity of both encoders and decoders. A cyclic or quasi-cyclic form of finite geometry LDPC codes simplifies the encoding procedure. In addition, the complexity of an iterative decoder for such codes, namely the min-sum algorithm, is lower than the complexity of a turbo or Reed–Solomon decoder. In fact, simple hard-decoding algorithms such as the bit-flipping algorithm perform very well on codes from projective planes. In this paper, the authors consider LDPC codes from affine planes, projective planes, oval designs, and unitals. The bit-error-rate (BER) performance of these codes is significantly better than that of any other known foward-error correction techniques for optical communications. A coding gain of 9–10 dB at a BER of $10^{-9}$, depending on the code rate, demonstrated here is the best result reported so far. In order to assess the performance of the proposed coding schemes, a very realistic simulation model is used that takes into account in a natural way all major impairments in long-haul optical transmission such as amplified spontaneous emission noise, pulse distortion due to fiber nonlinearities, chromatic dispersion, crosstalk effects, and intersymbol interferencec. This approach gives a much better estimate of the code's performance than the commonly used additive white Gaussian noise channel model.**

***Index Terms*—Finite geometries codes, forward-error correction (FEC), low-density parity-check (LDPC) codes, optical communications.**

## I. Introduction

DENSE-wavelength-division-multiplexing (DWDM) fiber optics communication becomes the predominant transport mechanism for metropolitan, wide-area networks, and long-haul transmission. The technologies enabling 40-Gb/s/ch wavelength-division-multiplexing (WDM) transmissions have been recently extensively studied. However, before the 40-Gb/s/ch WDM systems become reality, a number of problems must be overcome: increased sensitivity to accumulated chromatic dispersion, dispersion slope, polarization-mode dispersion (PMD), increased sensitivity to fiber nonlinearities, amplified spontaneous emission (ASE) noise accumulation, double-Rayleigh backscattering in Raman amplifier applications, etc. The main approach applied in long-haul communications is to reduce and tolerate the fiber nonlinearities so that the system operates in the so-called *quasi-linear regime* [1]. For such applications, the role of the proper modulation scheme, proper dispersion map, and proper forward-error correction (FEC) schemes [1], [2] are increasingly important to maintain the acceptable transmission system performance.

Ait Sab proposed a concatenated scheme with two Reed–Solomon (RS) codes and another scheme with block turbo codes (BTCs) [3]–[5]. In a series of recent articles, we showed that error performance and decoder hardware complexity offered by turbo codes can be greatly improved by using other types of iteratively decodable coding schemes, in particular low-density parity-check (LDPC) codes [2], [6]. The LDPC codes have been shown to perform approximately within 0.005 dB of the Shannon limit on an additive white Gaussian noise (AWGN) channel (rate 1/2, codeword size of $10^7$) [7], breaking the record previously set by turbo codes. Moreover, Hagenauer *et al.* [9] realized that the sum-product algorithm is well suited for analog very-large-scale-integration (VLSI) implementation. This kind of fast analog iterative decoder is a very attractive option for future optical communications. Although LDPC codes can be designed in a pseudorandom fashion [8], such codes may lead to encoders/decoders so complex that it is impractical to employ them in high-speed optical communications. High-speed FEC architectures are critical in optical communications, and there has been a great deal of research interests in this area. For example, Agere Systems have reportedly built an optical networking interface device with four parallel RS codecs, each operating at 2.5 Gb/s [28]. Several well-known systematic construction methods for LDPC codes [2], [6], [17], [25] provide parity-check matrices with cyclic or quasi-cyclic structures, thereby reducing the hardware complexity of LDPC encoders and decoders.

In [2], [6], and [25], we presented systematic LDPC code constructions based on rectangular lattices, mutually orthogonal Latin squares, and projective geometry (PG), respectively. These codes have many favorable features, namely high code rate and large minimum distance, and they support simple encoders, realized using shift registers, and simple iterative decoding algorithms.

In [25], we presented a systematic LDPC code construction based on the point-line incidence matrix of a projective plane. The number of distinct codes (obtained from this construction) that are relevant to WDM high-speed long-haul transmission systems is limited. The flexibility of code construction can be increased by investigating secondary structures in projective

Manuscript received April 24, 2003; revised November 30, 2003. This work is supported by the National Science Foundation (NSF) under Grant ITR 0325979.

I. B. Djordjevic is with the University of Arizona, Tucson, AZ 85721 USA, on leave from the University of the West of England, Bristol BS16 1QY, U.K. (e-mail: ivan@ece. arizona.edu).

S. Sankaranarayanan and B. V. Vasic are with the Department of Electrical and Computer Engineering, University of Arizona, Tucson AZ 85721 USA (e-mail: ssundar@ece.arizona.edu; vasic@ece.arizona.edu).

Digital Object Identifier 10.1109/JLT.2004.825768

planes and also by using the point-line incidence structure of the affine plane. In the following subsections, we present details of the construction of LDPC codes from affine geometry (AG), PG, oval designs, and unitals. In addition, we present some encouraging preliminary results, which show that these codes, with a coding gain of 10 dB at BER of $10^{-9}$, significantly outperform any other FEC techniques, including the turbo codes, reported so far. The coding gains larger from that reported in Section IV ($\sim$10 dB at BER of $10^{-9}$) are possible for PG(2,64) and PG(2,128) (as well as with oval and unital designs of comparable code rates, lengths, and minimum distance) since the corresponding minimum distances are at least 66 and 130, respectively.

A very realistic simulation model that takes into account all major impairments in long-haul optical transmission (such as ASE noise, pulse distortion due to fiber nonlinearities, chromatic dispersion, crosstalk effects, and intersymbol interference (ISI)) is used in experiments because it is a better approximation of the realistic optical channel than the commonly used AWGN channel model.

## II. Finite Geometry Codes

The code constructions proposed in this paper are based on the theory of combinatorial designs. A*balanced incomplete block design* (BIBD) is defined as a collection of $k$ subsets of a $v$ set $S$, $k < v$, such that pair of elements of $S$ occurs together in exactly $\lambda$ blocks. Each $k$ subset is called a *block*, and each element of $S$ is called a *point*. The design is said to be *balanced* because each pair of elements of $S$ occur together in exactly $\lambda$ blocks, and it is said to be *incomplete* because not all possible $k$ subsets of $S$ are elements of the set of blocks. A BIBD is referred to as a design with parameters $2-(v,k,\lambda)$. Further details about designs in general and BIBD in specific can be found in [10]–[17]. The *incidence matrix* of a $2-(v,k,\lambda)$ design with $b$ blocks is a $b \times v$ matrix $A=(a_{ij})$ defined by

$$a_{ij} = \begin{cases} 1, & \text{if the } i\text{th block contains the } j\text{th point} \\ 0, & \text{otherwise.} \end{cases}$$

The parity-check matrix ($\boldsymbol{H}$) of an LDPC code from a BIBD is the transpose of its incidence matrix $\boldsymbol{A}$. A BIBD is *resolvable* if the blocks can be partitioned into $r = bk/v$ groups such that each group contains blocks whose pairwise intersection is a disjoint set, and their union is the set of points $S$. The groups are called the *resolution classes* or the *parallel classes*. Interpreting geometrically, a resolution class can be viewed as a collection of parallel lines.

A finite projective plane (geometry) [14] of order $n$, say PG(2, $n$), is an $2-(n^2+n+1, n+1, 1)$ design, $n \geq 2$, and $n$ is a power of prime. The point set of the design consists of all the *points* on PG(2, $n$), and the block set of the design consist of all *lines* on PG(2, $n$). The points and lines of a finite projective plane satisfy four sets of axioms.

1) Every line consists of the same number of points.
2) Any two points on the plane are connected by a unique line.
3) Any two lines on the plane intersect at a unique point.
4) A fixed number of lines pass through any point on the plane.

As mentioned previously, since any two lines on a projective plane intersect at a unique point, there are no parallel lines on the plane. The incidence matrix of such a design, for $n=2^m$, is cyclic and, hence, any row of the matrix can be obtained by shifting (right or left) another row of the matrix.

A finite affine plane of order $n$, say AG(2, $n$), is a $2-(n^2, n, 1)$ design, $n \geq 2$ and $n$ is a power of prime. A finite affine plane of order $n$, is a special case of a finite projective plane of the same order. One of the main differences between a PG(2, $n$) and AG(2, $n$) is that any two lines on the affine plane may or may not intersect. This difference between an AG(2, $n$) and a PG(2, $n$) introduces the concept of *parallelism* in the affine plane. An affine plane AG(2, $n$) can be constructed by "discarding" all the points of a line in PG(2, $n$), and this "discarded" line is usually referred to as the *line at infinity*. Hence, the number of lines (blocks) is one less than that in PG(2, $n$), and each line (block) has one less point than that in PG(2, $n$).

Ovals and unitals [12]–[15] are special geometrical structures, namely *arcs*, on a projective plane. In other words, these arcs, defined on a projective plane, help to construct new subdesigns by "discarding" a selected set of points and lines on the plane. In PG(2, $n$), any non-empty set of $r$ points is a $\{r; m\}$ *arc*, $m \neq 0$, where $m$ is the greatest number of collinear points in the set. The parity-check matrices of codes from such designs exhibit quasi-cyclic properties. A *hyperoval* on a PG(2, $n$), $n$ even, is a $\{n+2, 2\}$ arc, and this can be constructed by extending a $\{n+1, 2\}$ arc with a uniquely defined point called the *nucleus* of the arc. The lines of the plane PG(2, $n$) can be divided into three classes with respect to the hyperoval.

1) A *tangent* is a line that meets the arc in a unique point.
2) A *secant* is a line that meets the arc in exactly two points.
3) An *exterior line* is a line that does not meet the arc.

The *nucleus* of a hyperoval is a unique point through which all tangents of the arc pass through. A hyperoval can be characterized algebraically as a set of points that satisfy an irreducible conic along with the nucleus of the arc. An *irreducible conic* is a homogeneous algebraic function of second order that is irreducible in the Galois field of order $n$. In PG(2, $n$), for $n=2^m$, an *oval design* is the incidence having the lines exterior to the hyperoval for *points*, and for *blocks*, the points not on the hyperoval. The oval design is a $2-(n(n-1)/2, n/2, 1)$ BIBD whose incidence matrix has a 2 rank of $3^m - 2^m$. In addition, the oval design is a resolvable design. The parity-check matrix of an LDPC code constructed from the oval design is defined as the transpose of the incidence matrix of the design.

A *Hermitian arc* or a *unital* in PG(2, $n$), $\sqrt{n}$ is an integer, is a $\{n\sqrt{n}+1, \sqrt{n}+1\}$ arc such that any line of the projective plane intersects the arc in either one or $\sqrt{n}+1$ points. A line meeting the unital in a single point is called the *tangent*. A unital can be characterized algebraically as a set of points that satisfy an irreducible homogeneous function of order $\sqrt{n}+1$. The Hermitian arc, together with the nontangent lines in PG(2, $n$), form a $2-(n\sqrt{n}+1, \sqrt{n}+1, 1)$ BIBD. The rank of an incidence matrix of the design is $(\sqrt{n})^3$, if $n$ is a power of 2, and $[(\sqrt{n})^2 - \sqrt{n} + 1]\sqrt{n}$, if $n$ is a power of odd prime [13], [15]. The parity-check matrix of an LDPC code constructed from the unital design is defined as the transpose of the incidence matrix of the design.

In a finite geometry, no two distinct lines can intersect at more than one distinct point. Hence, an LDPC code from a finite geometry is orthogonal and can be decoded by a number of algorithms such as one-step majority-logic decoding, bit flipping (BF), weighted bit flipping, and message passing. Although sum-product iterative decoding has been demonstrated to perform well in various types of channels, it is computationally intensive, and it is not clear if it is suitable for optical communications at data rate 40 Gb/s or higher. However, the *min-sum* version of this *algorithm* (MSA) (see Appendix A), [18], [24], [26]–[28] which is an approximation of *a posteriori* probability decoding, requires only simple addition and "finding minimum" operations and, as such, is suitable for high-speed optical transmission. One advantage of these codes is that the code parameters, such as minimum distance and bipartite graph girth, are easily controllable. These features are the result of the highly regular structures of these codes.

In Table I, we have listed design parameters of families of finite geometry codes presented in this paper. Fig. 1 shows the code length as a function of code rate for LDPC codes obtained by using finite geometry codes. If required code rate is higher than 0.8, the typical requirement for optical communications, it is impossible to construct code shorter than 500. The codes based on PG($m, p^s$), proposed in [25], are more general than the projective plane codes (the first row of Table I), and the underlying mathematics is more complicated. However, the number of codes with different code rates is rather limited. For example, it is evident from Fig. 1 that just three codes from the projective plane (i.e., for $m = 5, 6, 7$) are applicable to optical communications. Novel constructions derived from projective planes (such as affine plane, ovals, and unitals) are required to increase the number of codes (with different code rates) applicable to optical communications.

*Example:* The parity-check matrix $H$ of a code from a hyperoval in PG(2,2) is

$$\boldsymbol{H} = \begin{bmatrix} 1 & 0 & 0 & 0 & 0 & 1 & 0 & 0 & 1 & 0 & 0 & 1 & 0 & 0 & 1 \\ 1 & 0 & 0 & 0 & 1 & 0 & 0 & 1 & 0 & 0 & 1 & 0 & 0 & 1 & 0 \\ 0 & 1 & 0 & 1 & 0 & 0 & 0 & 0 & 1 & 0 & 1 & 0 & 1 & 0 & 0 \\ 0 & 0 & 1 & 0 & 1 & 0 & 1 & 0 & 0 & 0 & 0 & 1 & 1 & 0 & 0 \\ 0 & 0 & 1 & 1 & 0 & 0 & 0 & 1 & 0 & 1 & 0 & 0 & 0 & 0 & 1 \\ 0 & 1 & 0 & 0 & 0 & 1 & 1 & 0 & 0 & 1 & 0 & 0 & 0 & 1 & 0 \end{bmatrix}.$$

Since any two points are connected by one and only one line, no two rows or columns have more than one "1" in common. Therefore, the point-line incident matrix is in fact the parity-check matrix of the LDPC code, and the corresponding Tanner graph is free of cycles of length 4.

Finding the minimum distance of BIBD codes is still an unsolved problem. However, it can be shown that a lower bound on minimum distance is $k + 1$. (The reader is referred to [22] for the proof.) For $n = 2^m$ $(m \geq 1)$, we have listed in Table II the lower bounds on minimum distance and the expected ranks of the parity-check matrix (the number of parity bits) for different finite geometry codes considered here. For example, the codes on oval(2,64) and AG(2,32) have the minimum distance of at least 33, while the code on PG(2,32) at least 34. Large minimum distance and factor graphs with good cycle properties result in excellent BER performance, shown in Section IV.

TABLE I
FINITE GEOMETRY $2-(v,k,1)$ FAMILIES

| $k$ | $v$ | Parameter | Name |
|---|---|---|---|
| $n+1$ | $n^2+n+1$ | $n$- a prime power | Projective planes |
| $n$ | $n^2$ | $n$- a prime power | Affine planes |
| $n/2$ | $n(n-1)/2$ | $n$- a prime power and even | Oval designs |
| $\sqrt{n}+1$ | $n\sqrt{n}+1$ | $n$- a prime and square | Unitals |

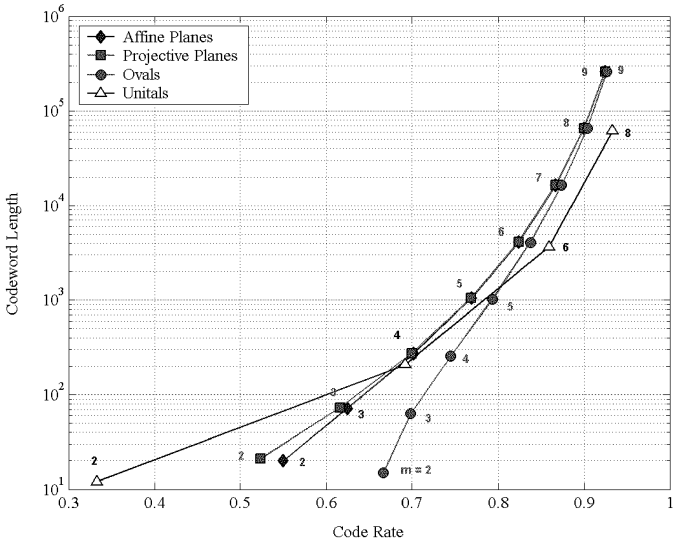


Fig. 1. Required codeword lengths of finite geometry codes ($n = 2^m$, $m \geq 2$).

## III. SIMULATION MODEL DESCRIPTION

In WDM systems, multiple optical carriers at different wavelengths are modulated by using independent electrical signals and then transmitted over the same fiber. The optical signal at the receiver is split into separate channels by using an optical demultiplexer. Erbium-doped fiber amplifiers (EDFAs) and dispersion-compensating fibers (DCFs) are deployed periodically to compensate the loss and accumulated dispersion of the standard single-mode fiber (SMF). A carrier-suppressed return-to-zero (CSRZ) modulator, considered here, is composed of a laser diode, a Mach–Zehnder (MZ) intensity modulator, another MZ modulator driven by a sinusoid at half-bit-rate frequency, and an encoder. A typical direct-detection receiver is composed of a polarization filter, an optical filter of the transfer function $H_1(f)$ (and impulse response $h_1(t)$), a p-i-n photodiode, an electrical filter of the transfer function $H_2(f)$ (and impulse response $h_2(t)$), a sampler and a decision circuit, followed by a decoder. ($H_1(f)$ may represent the transfer function of the WDM demultiplexer (e.g., the AWG), and $H_2(f)$ the transfer function of complete receiver electronics.)

The propagation of a signal through the transmission media is modeled by the nonlinear Schrödinger equation [19]

$$\frac{\partial A}{\partial z} = -\frac{\alpha}{2} - \frac{i}{2}\beta_2 \frac{\partial^2 A}{\partial T^2} + \frac{\beta_3}{6}\frac{\partial^3 A}{\partial T^3} + i\gamma\left(|A|^2 - T_R\frac{\partial |A|^2}{\partial T}\right)A \quad (1)$$

TABLE II
PARITY-CHECK MATRICES RANKS AND LOWER BOUND ON MINIMUM DISTANCE OF FINITE GEOMETRY CODES

| Geometry | Parity-check matrix rank | Lower-bound on minimum-distance |
|---|---|---|
| Projective planes | $3^m+1$ | $2^m+2$ |
| Affine planes | $3^m$ | $2^m+1$ |
| Oval designs | $3^m-2^m$ | $2^{m-1}+1$ |
| Unitals | $2^{3m/2}$ | $2^{m/2}+2$ |

where $z$ is the distance propagated along the fiber, relative time $T = t - z/v_g$ gives a frame of reference moving at the group velocity $v_g$, $A(z,T)$ is the complex field amplitude of the pulse, $\alpha$ is the attenuation coefficient of the fiber, $\beta_2$ is the group-velocity dispersion (GVD) coefficient, $\beta_3$ is the second-order GVD, $\gamma$ is the nonlinearity coefficient giving rise to Kerr effect nonlinearities, and $T_R$ is the Raman coefficient. Equation (1) is solved using the split-step Fourier method, as described in [19].

The electrical field coming through the fiber to the optical filter input can be written as

$$r(t) = s(t) + n(t), s(t) = \sum_{n=-\infty}^{\infty} \sqrt{b_n P} p_n(t - nT_b) \quad (2)$$

where $s(t)$ is the (optical) amplifier chain output signal field. (Notice that the propagation of the signal is considered separatly from the ASE noise in order to improve the speed of the simulation. The justification of such an approach, valid for quasilinear system considered here, is discussed in [23].) In (2), $p_n(t)$ is the $n$th bit pulse shape, $P$ is the peak power, and $b_n$ is the (coded) information content $b_n \in \{r, 1\}$, with $r$ being the extinction ratio $0 \leq r < 1$. Both the ASE noise components and the multipath interference (MPI) components are combined into a noise process $n(t)$, which is considered to be colored Gaussian with autocorrelation function given by

$$R_n(\tau) = R_{\mathrm{ASE}}(\tau) + R_{\mathrm{MPI}}(\tau) \quad (3)$$

($R_{\mathrm{ASE}}(\tau)$ and $R_{\mathrm{MPI}}(\tau)$ are ASE and MPI autocorrelaction functions, respectively). The power spectral density of ASE noise is determined by the EDFA output filter, and the spectrum of MPI noise is determined by the signal spectrum. The autocorrelation function of ASE noise is $R_{\mathrm{ASE}}(\tau) = N_0 R_{\mathrm{EDFA}}(\tau)$, where $R_{\mathrm{EDFA}}(\tau)$ is the EDFA output optical filter autocorrelation function, and $N_0$ is the power spectral density of ASE noise in one state of polarization. Within the bandwidth of an optical filter in EDFA, the noise power spectral density function can be approximated as $N_0 \approx n_{\mathrm{sp}}(G-1)hf\ N_{\mathrm{amp}}$, wherein $n_{\mathrm{sp}}$ is the spontaneous emission factor, $G$ is the EDFA gain, $hf$ is the photon energy, and $N_{\mathrm{amp}}$ is the number of amplifiers. $r(t)$, $s(t)$, and $p_n(t)$ are in fact the complex envelopes of corresponding analytical signals.

The photodiode output noise process has the mean

$$\overline{I(t)} = \int_{-\infty}^{\infty} |S(\tau)|^2 h_2(t-\tau) d\tau + R_N(0) \quad (4)$$

and the variance

$$\begin{aligned}\sigma^2(t) = 2R_e \Bigg\{ &\int_{-\infty}^{\infty}\int_{-\infty}^{\infty} S(\tau) S^*(\hat{\tau}) R_N(\tau - \hat{\tau}) \\ &\times h_2(t-\tau) h_2(t-\hat{\tau}) d\tau d\hat{\tau} \Bigg\} \\ &+ 2 \int_{-\infty}^{\infty}\int_{-\infty}^{\infty} h_2(t-\tau) \left| R_N(\tau - \hat{\tau}) \right|^2 \\ &\times h_2(t-\tau) d\tau d\hat{\tau} + q\overline{I(t)} + \sigma_e^2 \end{aligned} \quad (5)$$

where $S(t) = s(t) * h_1(t)$ is the optical filter output signal. (The derivation of the expressions (4) and (5) is given in our previous paper [20].) The autocorrelation function of the optical filter output noise can be expressed as

$$R_N(\tau) = \int_{-\infty}^{\infty} R_{h_1}(t) R_n(\tau - t) dt \quad (6)$$

where $R_{h_1}(\tau)$ is the optical filter autocorrelation function. Notice that the photodiode output noise process is not stationary (the mean values and the standard deviation are functions of time). In (5), $\sigma_e^2$ is the electronic noise variance, which includes both transmitter and receiver electronic noise (also known as "back-to-back" noise), while $q\bar{I}$ is the photodiode shot-noise variance ($q$ is an electron charge). If the polarization filter is omitted, the second term in (5) should be multiplied by a factor of two. In optical communications, it is a custom to use a $Q$ factor [21] as a figure of merit rather than signal-to-noise ratio, and in this paper, we will follow this convention.

Using the expression in (7), the BER of uncoded signal

$$\mathrm{Uncoded\_BER} = \left(\frac{1}{2}\right) \mathrm{erfc}\left(\frac{Q}{\sqrt{2}}\right) \quad (7)$$

is converted to $Q$ factor in order to make the results comparable with previously reported ones. (Since the code rate influence is included in the $Q$ factor, the reported coding gain is equivalent to the net effective coding gain of AWGN channel.)

In simulations, the pseudorandom bit sequence (PRBS) of length $2^{15} - 1$ is encoded and transmitted over transmission media. The parameters required in (4) and (5) are determined at the end of the transmission media, and then such obtained sequence is repeated for different ASE noise realizations. The validity of considering ASE noise independently of the transmitted signal, the assumption valid for the quasi-linear systems, is discussed in [23]. (We have found the excellent agreement between the BER of the uncoded signal with

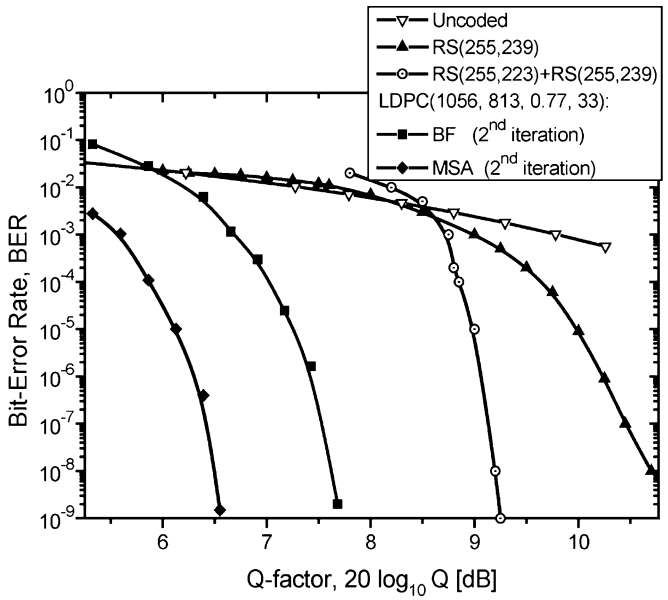


Fig. 2. BER versus $Q$ factor for AG(2, $2^5$)-based LDPC code at 10 Gb/s.

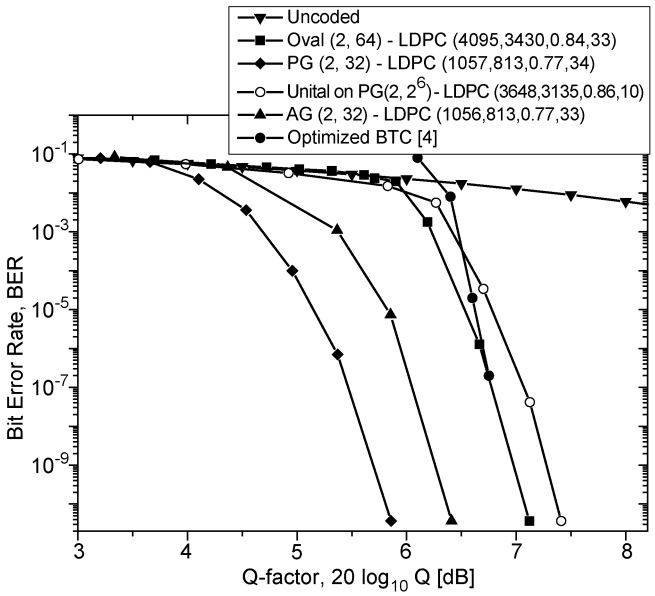


Fig. 3. BER performance of AG(2, $2^5$)-, PG(2, $2^5$)-, oval(2, $2^6$)-, and unital on PG(2, $2^6$)-based LDPC codes at 40 Gb/s (after the third iteration).

overhead included and the BER calculated from the undecoded signal.) ASE noise samples are added to the signal (processed according to (4)) as a zero-mean nonstationary Gasussian process of variance (5)—the variance is different from sample to sample. The validity of such an approach is discussed in our previous paper [20], where overlapping results with Monte Carlo simulations are obtained. (Notice that the process generated in such a way is nonstationary (5).) The simulator developed allows also to transmit the encoded signal when ASE noise—signal interaction during transmission over the fiber media is included, which is unavoidable in a highly nonlinear transmission system. Unfortunately, the simulation for such a system will be unacceptably long. Similarly, as in [23], the back-to-back $Q$ factor is included as the AWGN contribution, with variance determined from the measured back-to-back $Q$ factor.

## IV. Finite Geometry Codes Performance

In this section, we present the BER performance of finite geometries (affine and projective geometries, oval designs, and unitals) LDPC codes in the presence of residual dispersion, fiber nonlinearities, ISI, and receiver noise resulting from signal–noise and noise–noise interaction on a photodiode. Transfer functions of optical and electrical filters are also taken into account. A WDM system with a 10- or 40-Gb/s bit rate per channel and a channel spacing of 50 or 100 GHz, respectively, is considered. It is assumed that the observed channel is located at 1552.524 nm or 193.1 THz and that there exists a nonnegligible interaction with six neighboring channels.

The performance of an affine geometry based LDPC (1056, 813, 0.77, 33) code (the last two parameters denote the code rate and the lower bound on minimum distance) with a code rate of $R = 0.7699$ (redundancy of ≈30%), for AG(2,32) ($b = 1056$) is shown in Fig. 2. The nonreturn-to-zero (NRZ) signal format at 10 Gb/s (per channel) is observed. The receiver comprised of an EDFA as a preamplifier, an optical filter (modeled as super-Gaussian filter of the eight order and bandwidth $2R_b$, $R_b$ bit rate over code rate), a p-i-n photodiode, an electrical filter (modeled as a Gaussian filter of bandwidth $0.65R_b$), a sampler, and a decision circuit are observed. Transmission with a dispersion map composed of standard SMF and DCF sections giving the residual dispersion of 272 ps/nm is considered. The SMF and DCF parameters are the same as in our previous paper [2]. An average power per channel of 0 dBm is assumed. The extinction ratio is set to 13 dB. The transmitter and receiver imperfections are described through a back-to-back $Q$ factor, which is set to 23 dB. For a BER value of $10^{-9}$, the LDPC (1056, 813) scheme with simple bit-flipping decoding outperforms the conventional RS(255 223)+RS(255 239) concatenation scheme by more than 1.5 dB, while the soft-decision variant based on the min-sum algorithm is better by 2.7 dB. It also outperforms the much more complex BTC based on a product of two Bose–Chaudhuri–Hocquenghem (BCH) (128, 113, 6) codes (with five iterations and comparable redundancy of 28%) by 0.5 dB.

Fig. 3 shows the BER results of a Monte Carlo simulation for a PG-based LDPC (1057, 813, 0.77, 34) code with a code rate of $R = 0.769$ (redundancy of ≈30%), oval-design-based code with a code rate 0.8376 (redundancy of 19%),a code based on a unital on PG(2, $2^6$) with s code rate 0.8594 (redundancy of 11.6%), and s code based on AG(2,$2^5$) for CSRZ modulation format at 40 Gb/s. The transmission system considered has a dispersion map composed of an SMF section, followed by an EDFA to compensate the fiber losses in the SMF section, and a DCF section to compensate both GVD and second-order GVD, as well as another EDFA to compensate fiber losses in the DCF section. (The SMF attenuation coefficient, dispersion, dispersion slope, nonlinear refractive index, and effective cross-sectional area are set to 0.22 dB/km, 16 ps·nm$^{-1}$ · km$^{-1}$, 0.08 ps·nm$^{-2}$ · km$^{-1}$, $2.6 \cdot 10^{-20}$ m$^2$/ W and 80 $\mu$m$^2$, respectively. Corresponding DCF parameters are 0.5 dB/km, −90 ps · nm$^{-1}$ · km$^{-1}$, −0.45 ps · nm$^{-2}$ · km$^{-1}$, $2.6 \cdot 10^{-20}$ m$^2$/ W, and 30 $\mu$m$^2$.) A coding gain of approximately 10 dB at a BER of $10^{-9}$ is better than that of any other coding scheme proposed

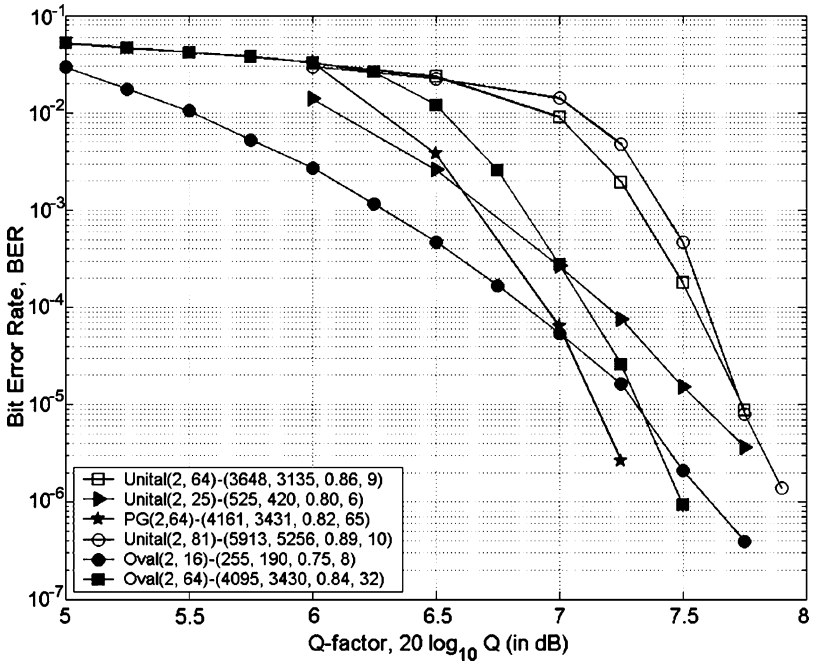


Fig. 4. Projected BER performance of unital on PG(2, 64)-, PG(2, 81)-, PG(2, 25)-, and PG(2, 64)-based LDPC codes on AWGN channel, and projected BER performance of oval on PG(2, 16)- and PG(2, 64)-based LDPC codes on AWGN channel.

so far. A PG-based LDPC (1057, 813, 0.77, 34) code outperforms the BTC based on a product of two BCH (128, 113, 6) codes (with five iterations and comparable redundancy of 28%) [4] (also included in Fig. 3) by 1 dB, while a code from a hyperoval in PG(2,64) with lesser redundancy (19%) and a code from a unital with redundancy of 11.6% have comparable performances. The AG codes perform slightly worse than PG codes. It is important to note that the complexity of the decoding algorithm, the min-sum algorithm, is at least one order simpler than that of the turbo decoder because these codes do not require any interleavers. For more details on hardware implementation of high-throughput LDPC codes, the reader is referred to [26]. The implementation of a variant of the min-sum algorithm is discussed in [27].

The comparison among different finite geometry codes for the AWGN channel model may be made from Fig. 4. As in an optical channel, the projective plane codes perform the best, since the minimum distance is the largest. The prediction on the performance of finite geometry codes made from AWGN channel is too pessimistic (although the more complex algorithm, the sum-product with 15 iterations, is employed). The choice of dispersion map, as can be seen by comparing AG(2,32) code performance in Figs. 2 and 3, also influences the FEC efficiency. Therefore, the AWGN channel may be used just as an initial prediction of FEC performance.

From Figs. 3, 4, it is evident that short codes of small minimum distance (oval(2,16) and oval(2,25)) experience the error floor. The longer codes of small minimum distance (unital(2,64)) do not experience the error floor down to $10^{-10}$. We believe that medium length, and especially long, finite geometry codes of large minimum distance will not experience the error floor down to $10^{-15}$. Since this claim cannot be supported by simulations, the error-floor of LDPC codes remains an open issue for further research.

## V. Conclusion

A novel class of FEC for long-haul optical communication systems based on finite geometry (affine and projective planes, oval designs, and unitals) LDPC codes and iterative decoding is presented in this paper. As opposed to recent papers [3]–[5] where the AWGN assumption is applied, we consider the performance of finite geometry codes in the presence of ASE noise, pulse distortion due to fiber nonlinearities, residual dispersion, crosstalk effects, ISI, etc. The iterative decoding based on a normalized min-sum algorithm has been demonstrated to give a coding gain of 9–10 dB, depending on the code rate and family, at a BER of $10^{-9}$. These codes have many unique features (e.g., high code rate, large minimum distances, and simple decoding algorithms and the encoder can be realized using shift registers) that may allow for very-high-speed implementations.

Since our extensive simulations show that the finite geometry LPDC codes perform well in the presence of all the previously mentioned impairments and significantly outperform previously proposed FEC schemes [3]–[5], including the turbo codes, we are confident in proposing their use in optical communications for high-speed long-haul transmission.

## Appendix A
## Min-Sum Decoding Algorithm

For any codeword $x = (x_v)_{1\le v\le n}$ in a linear block code given by the parity-check matrix $\boldsymbol{H}$, the following set of equations is satisfied

$$\sum_v h_{c,v}x_v = 0, \quad 1 \le c \le n-k. \tag{A1}$$

These equations are called parity-check equations. Iterative decoding can be visualized as message passing on a bipartite graph

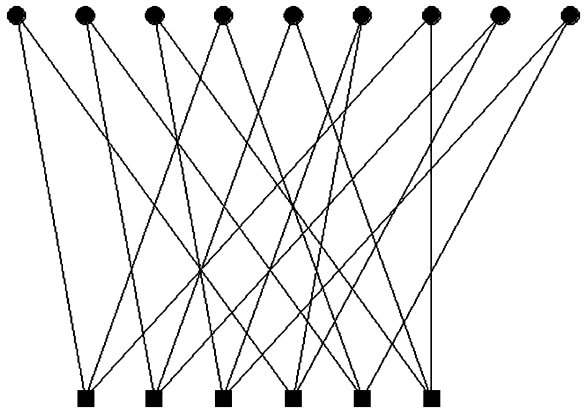

Fig. 5. Example of a bipartite graph.

representation, called *Tanner graph*, of the parity-check matrix [22]. There are two types of vertices in the graph: check vertices (check nodes) indexed by $c$, and variable vertices (bit nodes) indexed by $v$. Edge-connecting vertices $c$ and $v$ exist if $h_{c,v} = 1$, i.e., if variable $v$ participates in the parity-check equation $c$. For example, the bipartite graph corresponding to

$$\boldsymbol{H} = \begin{bmatrix} 1 & 0 & 0 & 1 & 0 & 0 & 1 & 0 & 0 \\ 0 & 1 & 0 & 0 & 1 & 0 & 0 & 1 & 0 \\ 0 & 0 & 1 & 0 & 0 & 1 & 0 & 0 & 1 \\ 1 & 0 & 0 & 0 & 0 & 1 & 0 & 1 & 0 \\ 0 & 1 & 0 & 1 & 0 & 0 & 0 & 0 & 1 \\ 0 & 0 & 1 & 0 & 1 & 0 & 1 & 0 & 0 \end{bmatrix}$$

is shown in Fig. 5. The check nodes are denoted by squares and the variable nodes by circles.

Decoding can be done as follows. First, *a priori* information of the bit at position $v$, $\mu_v^{(0)}$, is taken as the channel sample, and messages passed from node $v$ to node $c$ in the bipartite graph, $\lambda_{v,c}^{(0)}$, are initialized to $\mu_v^{(0)}$. In the $j$th iteration, we update the messages to be passed from the check node $c$ to the bit node $v$, $\Lambda_{c,v}^{(j)}$, as

$$\Lambda_{c,v}^{(j)} = \prod_{w \neq v} \operatorname{sign}\left(\lambda_{v,c}^{(j-1)}\right) \cdot \min_{w \neq v} \left|\lambda_{v,c}^{(j-1)}\right| \tag{A2}$$

and messages to be passed from bit node $v$ to check node $c$, $\lambda_{v,c}^{(j)}$, according to

$$\lambda_{v,c}^{(j)} = \mu_v^{(0)} + \sum_{d \neq c} \Lambda_{d,v}^{(j)}. \tag{A3}$$

The last step in iteration $j$ is to compute updated normalized log-likelihood ratios $\mu_v^{(j)}$ according to

$$\mu_v^{(j)} = \mu_v^{(0)} + \sum_{c} \Lambda_{c,v}^{(j)}. \tag{A4}$$

For each bit $x_v$, the estimation is made according to

$$\hat{x}_v = \begin{cases} 1, & \text{if } \mu_v^{(j)} < 0 \\ 0, & \text{otherwise} \end{cases}. \tag{A5}$$

Decoding halts when a valid codeword $\left(\sum_v h_{c,v}\hat{x}_v = 0\right)$ or when a maximum number of iteration has been reached. The steps (A2) and (A3) can be viewed as propagation of "beliefs" in a code bipartite graph [22].

## REFERENCES


[1] J. X. Cai, M. Nissov, C. R. Davidson, A. N. Pilipetskii, G. Mohs, H. Li, Y. Cai, E. A. Golovchenko, A. J. Lucero, D. G. Foursa, and N. S. Bergano, "Long-haul 40 Gb/s DWDM transmission with aggregate capacities exceeding 1Tb/s," *J. Lightwave Technol.*, vol. 20, pp. 2247–2258, Dec. 2002.

[2] B. Vasic and I. B. Djordjevic, "Low-density parity check codes for long haul optical communications systems," *IEEE Photon. Technol. Lett.*, vol. 14, pp. 1208–1210, Aug. 2002.

[3] O. Ait Sab, "FEC techniques in submarine transmission systems," in *Proc. Optical Fiber Communication Conf.*, vol. 2, 2001, pp. TuF1-1–TuF1-3.

[4] O. A. Sab and V. Lemarie, "Block turbo code performances for long-haul DWDM optical transmission systems," in *Proc. Optical Fiber Communication Conf.*, vol. 3, 2001, pp. 280–282.

[5] M. Akita, H. Fujita, T. Mizuochi, K. Kubo, H. Yoshida, K. Kuno, and S. Kurahashi, "Third generation FEC employing turbo product code for long-haul DWDM transmission systems," in *Tech. Dig. Optical Fiber Communication Exhibit*, 2002, pp. 289–290.

[6] B. Vasic, I. B. Djordjevic, and R. Kostuk, "Low-density parity check codes and iterative decoding for long haul optical communication systems," *J. Lightwave Technol.*, vol. 21, pp. 438–446, Feb. 2003.

[7] T. Richardson, A. Shokrollahi, and R. Urbanke, "Design of capacity-approaching irregular low-density parity-check codes," *IEEE Trans. Inform. Theory*, vol. 47, pp. 619–637, Feb. 2001.

[8] D. MacKay and M. Davey. Evaluation of Gallager Codes for Short Block Length and High Rate Applications. [Online] Available: http://www.cs.toronto.edu/~mackay/CodesRegular.html

[9] J. Hagenauer, M. Moerz, and E. Offer, "Analog turbo-networks in VLSI: The next step in turbo decoding and equalization," presented at the 2nd Int. Symp. Turbo Codes, Brest, France, Sept. 4–7, 2000.

[10] I. Andersen, "Combinatorial designs: Construction methods," in *Mathematics and Its Applications*. Chichester, U.K.: Ellis Horwood, 1990.

[11] *The Handbook of Combinatorial Designs*, C. J. Colbourn and J. H. Dinitz, Eds., CRC, Boca Raton, FL, 1996.

[12] J. A. Thas, *Handbook of Incidence Geometry: Buildings and Foundations*, F. Buekenhout, Ed. Amsterdam, The Netherlands: Elsevier Science, 1996, ch. 7.

[13] E. F. Assmus Jr. and J. D. Key, "Baer subplanes, ovals and unitals," in *Coding Theory and Design Theory, Part I*, D. Ray-Chaudhuri, Ed. New York: Springer-Verlag, 1990, vol. 20, The IMA Volumes in Mathematics and Its Applications, pp. 1–8.

[14] ——, *Designs and Their Codes*. Cambridge, U.K.: Cambridge Univ. Press, 1992.

[15] ——, "Designs and codes: An update," *Designs, Codes Cryptography*, vol. 9, pp. 7–27, 1996.

[16] Y. Kou, S. Lin, and M. P. C. Fossorier, "Low-density parity-check codes based on finite geometries: A rediscovery and new results," *IEEE Trans. Inform. Theory*, vol. 47, pp. 2711–2736, Nov. 2001.

[17] S. R. Weller and S. J. Johnson, "Iterative decoding of codes from oval designs," presented at the Defense Applications Signal Processing, 2001 Workshop (DASP2001), South Australia, Sept. 16–20, 2001.

[18] J. Hagenauer, E. Offer, and L. Papke, "Iterative decoding of binary block and convolutional codes," *IEEE Trans. Inform. Theory*, pp. 429–445, Mar. 1996.

[19] G. P. Agrawal, *Nonlinear Fiber Optics*. San Diego, CA: Academic, 2001.

[20] I. B. Djordjevic and B. Vasic, "An advanced direct detection receiver model," *J. Opt. Commun.*, vol. 20, no. 1, Feb. 2004.

[21] N. S. Bergano and C. R. Davidson, "Circulating loop transmission experiments for the study long-transmission systems using erbium-doped fiber amplifiers," *J. Lightwave Technol.*, vol. 13, pp. 879–888, May 1995.

[22] B. Vasic and O. Milenkovic, "Combinatorial constructions of structured low-density parity check codes for iterative decoding," *IEEE Trans. Inform. Theory*, to be published.

[23] E. A. Golovchenko, A. N. Pilipetskii, N. S. Bergano, C. R. Davidson, F. I. Khatri, R. M. Kimball, and V. J. Mazurczyk, "Modeling of transoceanic fiber-optic WDM communication systems," *IEEE J. Select. Topics Quantum Electron.*, vol. 6, pp. 337–347, Mar.–Apr. 2000.

[24] W. E. Ryan, "An introduction to LDPC codes," in *CRC Handbook for Coding and Signal Processing for Recording Systems*, B. Vasic, Ed. Boca Raton, FL: CRC, 2004, to be published.

[25] I. B. Djordjevic and B. Vasic, "Projective geometry low-density parity-check codes for ultra-long haul WDM high-speed transmission," *IEEE Photon. Technol. Lett.*, vol. 15, pp. 784–786, May 2003.

[26] E. Yeo, B. Nikolic, and V. Anantharam, "Iterative decoder architectures," *IEEE Commun. Mag.*, vol. 41, pp. 132–140, Aug. 2003.
[27] H. Xiao-Yu, E. Eleftheriou, D.-M. Arnold, and A. Dholakia, "Efficient implementations of the sum-product algorithm for decoding LDPC codes," in *Proc. IEEE GLOBECOM*, vol. 2, Nov. 2001, pp. 1036–1036E.
[28] K. Azadet, E. F. Haratsch, H. Kim, F. Saibi, J. H. Saunders, M. Shaffer, L. Song, and Y. MengLin, "Equalization and FEC techniques for optical transceivers," *IEEE J. Solid-State Circuits*, vol. 37, pp. 317–327, Mar. 2002.

**Ivan B. Djordjevic** received the Dipl.Ing., M.S., and Ph.D. degrees, all in electrical engineering, from the University of Nish, Nish, Serbia, in 1994, 1997, and 1999, respectively.

From 1994 to 1996, he was with the Faculty of Electronic Engineering, University of Nish, working on modeling and simulation of optical/digital communication systems. From 1996 to 2000, he was with the State Telecommunications Company (Serbia Telecom), District Office for Networks, Nish, Serbia, where he was involved in digital transmission systems commissioning and acceptance, design, maintenance, installation, and connection. From 2000 to 2001, he was with the National Technical University of Athens, Greece, and with TyCom US, Inc. (now TyCo Telecommunications), USA, where he was involved in modeling and simulation of dense-wavelength-division-multiplexing (DWMD) systems. During 2002 and 2003, he was with the University of Arizona, Tucson; the University of Bristol, U.K.; and the University of West of England, Bristol, U.K., working on forward-error correction and iterative decoding for optical transmission, optical CDMA, high-speed transmission, and optical switches. He is now with the University of Arizona, on leave from the University of West of England. He is an author of more than 35 international journal papers and more than 45 international conference papers. His research interests include DWDM fiber-optic communication systems and networks, FEC for optical communications, optical CDMA, optical packet switching, coding theory, coherent optical communications, and statistical communication theory.

**Sundararajan Sankaranarayanan** received the B.E. degree in electrical engineering from the University of Madras, India, and the M.S. degree in electrical engineering from the University of Arizona, Tucson. He is currently working toward the Ph.D. degree in digital communications at the Electrical and Computer Engineering Department, University of Arizona.

He was formerly with Philips Research, New York, and Seagate Research, Pennsylvania, in summers 2000 and 2002, respectively. His research interests include coding theory and its applications in magnetic recording systems and optical communication systems.

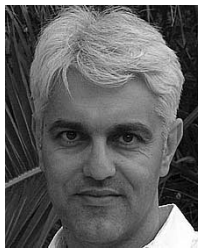

**Bane V. Vasic** (S'92–M'93–SM'02) received the B.S., M.S., and Ph.D. degrees in electrical engineering from the University of Nish, Serbia, Yugoslavia, in 1989, 1991, and 1994, respectively.

From 1996 to 1997, he was a Visiting Scientist at the Rochester Institute of Technology and Kodak Research, both in Rochester, NY, where he was involved in research on optical storage channels. From 1998 to 2000, he was with Lucent Technologies, where he was involved in research coding schemes and architectures for high-speed applications. He was also involved in iterative decoding and low-density parity check codes, as well as development of codes and detectors for five generations of Lucent (now Agere) chips. Currently, he is a Faculty Member of the Electrical and Computer Engineering Department, University of Arizona, Tucson. He has authored more than 25 journal articles, more than 50 conference papers, and more than six book chapters and one book. His research interests include coding theory, information theory, communication theory, digital communications, and recording.

Dr. Vasic is a Member of the Editorial Board of the IEEE TRANSACTIONS ON MAGNETICS. He served as Technical Program Chair of the IEEE Communication Theory Workshop 2003 and as Co-Organizer of the Center for Discrete Mathematics and Theoretical Computer Science (DIMACS) Workshops on Optical/Magnetic Recording and Optical Transmission and Theoretical Advances in Information Recording, 2004.